Designation: E 1268 – 9901

Standard Practice for Assessing the Degree of Banding or Orientation of Microstructures[1]

This standard is issued under the fixed designation E 1268; the number immediately following the designation indicates the year of original adoption or, in the case of revision, the year of last revision. A number in parentheses indicates the year of last reapproval. A superscript epsilon (ϵ) indicates an editorial change since the last revision or reapproval.

INTRODUCTION

Segregation occurs during the dendritic solidification of metals and alloys and is aligned by subsequent deformation. Solid-state transformations may be influenced by the resulting microsegregation pattern leading to development of a layered or banded microstructure. The most common example of banding is the layered ferrite-pearlite structure of wrought low-carbon and low-carbon alloy steels. Other examples of banding include carbide banding in hypereutectoid tool steels and martensite banding in heat-treated alloy steels. This practice covers procedures to describe the appearance of banded structures, procedures for characterizing the extent of banding, and a microindentation hardness procedure for determining the difference in hardness between bands in heat treated specimens. The stereological methods may also be used to characterize non-banded microstructures with second phase constituents oriented (elongated) in varying degrees in the deformation direction.

1. Scope

1.1 This practice describes a procedure to qualitatively describe the nature of banded or oriented microstructures based on the morphological appearance of the microstructure.

1.2 This practice describes stereological procedures for quantitative measurement of the degree of microstructural banding or orientation.

NOTE 1—Although stereological measurement methods are used to assess the degree of banding or alignment, the measurements are only made on planes parallel to the deformation direction (that is, a longitudinal plane) and the three-dimensional characteristics of the banding or alignment are not evaluated.

1.3 This practice describes a microindentation hardness test procedure for assessing the magnitude of the hardness differences present in banded heat-treated steels. For fully martensitic carbon and alloy steels (0.10–0.65 %C), in the as-quenched condition, the carbon content of the matrix and segregate may be estimated from the microindentation hardness values.

1.4 This standard does not cover chemical analytical methods for evaluating banded structures.

1.5 This practice deals only with the recommended test methods and nothing in it should be construed as defining or establishing limits of acceptability.

1.6 The measured values are stated in SI units, which are regarded as standard. Equivalent inch-pound values, when listed, are in parentheses and may be approximate.

1.7 *This standard does not purport to address all of the safety problems, if any, associated with its use. It is the responsibility of the user of this standard to establish appropriate safety and health practices and determine the applicability of regulatory limitations prior to use.*

2. Referenced Documents

2.1 *ASTM Standards:*

A 370 Test Methods and Definitions for Mechanical Testing of Steel Products[2]

[1] This practice is under the jurisdiction of ASTM Committee ~~E-4~~ E04 on Metallography and is the direct responsibility of Subcommittee E04.14 on Quantitative Metallography.

Current edition approved ~~April~~ Dec. 10, ~~1999.~~ 2001. Published ~~July 1999.~~ February 2002. Originally published as E 1268 – 88. Last previous edition E 1268 – 9~~4~~9.

A 572/A 572M Specification for High-Strength Low-Alloy Columbium-Vanadium Structural Steel[3]
A 588/A 588M Specification for High-Strength Low-Alloy Structural Steel with 50 ksi [345 MPa] Minimum Yield Point to 4 in. [100 mm] Thick[3]
E 3 Methods of Preparation of Metallographic Specimens[4]
E 7 Terminology Relating to Metallography[4]
E 140 Hardness Conversion Tables for Metals[4]
E 384 Test Method for Microhardness of Materials[4]
E 407 Test Methods for Microetching Metals and Alloys[4]
E 562 Practice for Determining Volume Fraction by Systematic Manual Point Count[4]
E 883 Guide for Reflected-Light Photomicrography[4]

3. Terminology

3.1 *Definitions*—For definitions of terms used in this practice, see Terminology E 7.

3.2 *Definitions of Terms Specific to This Standard:*

3.2.1 *banded microstructure*—separation, of one or more phases or constituents in a two-phase or multiphase microstructure, or of segregated regions in a single phase or constituent microstructure, into distinct layers parallel to the deformation axis due to elongation of microsegregation; other factors may also influence band formation, for example, the hot working finishing temperature, the degree of hot- or cold-work reduction, or split transformations due to limited hardenability or insufficient quench rate.

3.2.2 *feature interceptions*—the number of particles (or clusters of particles) of a phase or constituent of interest that are crossed by the lines of a test grid. (see Fig. 1).

3.2.3 *feature intersections*—the number of boundaries between the matrix phase and the phase or constituent of interest that are crossed by the lines of a test grid (see Fig. 1). For isolated particles in a matrix, the number of feature intersections will equal twice the number of feature interceptions.

3.2.4 *oriented constituents*—one or more second-phases (constituents) elongated in a non-banded (that is, random distribution) manner parallel to the deformation axis; the degree of elongation varies with the size and deformability of the phase or constituent and the degree of hot- or cold-work reduction.

[2] *Annual Book of ASTM Standards*, Vol 01.03.
[3] *Annual Book of ASTM Standards*, Vol 01.04.
[4] *Annual Book of ASTM Standards*, Vol 03.01.

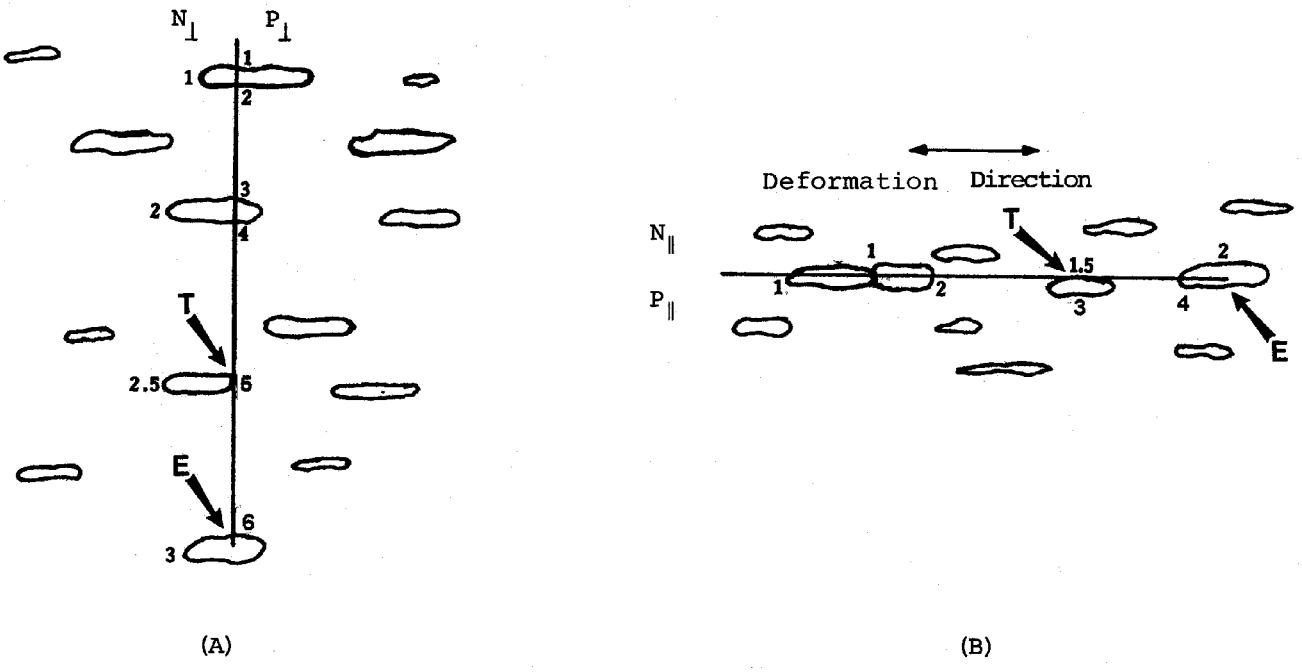

NOTE 1—The test grid lines have been shown oriented perpendicular (A) to the deformation axis and parallel (B) to the deformation axis. The counts for $N_{\perp}$, $N_{\parallel}$, $P_{\perp}$, and $P_{\parallel}$ are shown for counts made from top to bottom (A) or from left to right (B).
NOTE 2—*T* indicates a tangent hit and *E* indicates that the grid line ended within the particle; both situations are handled as shown.

FIG. 1 Illustration of the Counting of Particle Interceptions (N) and Boundary Intersections (P) for an Oriented Microstructure

3.2.5 *stereological methods*—procedures used to characterize three-dimensional microstructural features based on measurements made on two-dimensional sectioning planes.

NOTE 2—Microstructural examples are presented in Annex A1 to illustrate the use of terminology for providing a qualitative description of the nature and extent of the banding or orientation. Fig. 2 describes the classification approach.

3.3 *Symbols*:

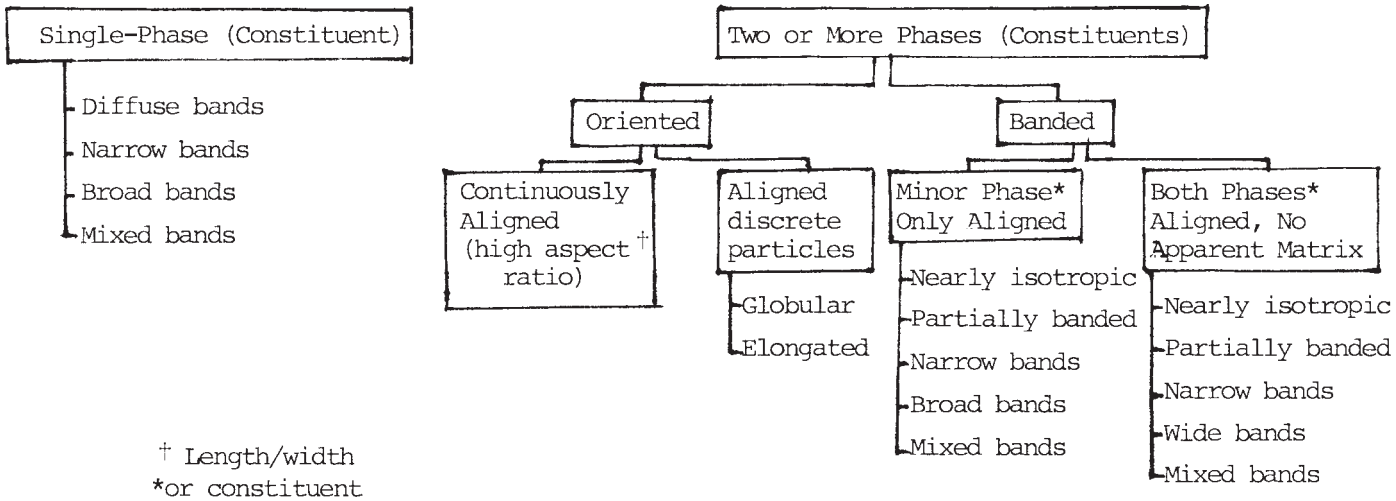

FIG. 2 Qualitative Classification Scheme for Oriented or Banded Microstructures

$N_{\perp}$ = number of feature interceptions with test lines perpendicular to the deformation direction.
$N_{||}$ = number of feature interceptions with test lines parallel to the deformation direction.
M = magnification.
L_t = true test line length in mm, that is, the test line length divided by M.
$N_{L\perp}$ = $\dfrac{N_{\perp}}{L_t}$

$N_{L||}$ = $\dfrac{N_{||}}{L_t}$

$P_{\perp}$ = number of feature boundary intersections with test lines perpendicular to the deformation direction.
$P_{||}$ = number of feature boundary intersections with test lines parallel to the deformation direction.
$P_{L\perp}$ = $\dfrac{P_{\perp}}{L_t} \cong 2N_{L\perp}$

$P_{L||}$ = $\dfrac{P_{||}}{L_t} \cong 2N_{L||}$

n = number of measurement fields or number of microindentation impressions.
$\bar{N}_{L\perp}$ = $\dfrac{\Sigma N_{L\perp}}{n}$

$\bar{N}_{L||}$ = $\dfrac{\Sigma N_{L||}}{n}$

$\bar{P}_{L\perp}$ = $\dfrac{\Sigma P_{L\perp}}{n} \cong 2\bar{N}_{L\perp}$

$\bar{P}_{L||}$ = $\dfrac{\Sigma P_{L||}}{n} \cong 2\bar{N}_{L||}$

$\bar{X}$ = mean values ($\bar{N}_{L\perp}$, $\bar{N}_{L||}$, $\bar{P}_{L\perp}$, $\bar{P}_{L||}$)
s = estimate of standard deviation (σ).
t = ~~Student t~~a multiplier related to the number of fields examined and used in conjunction with the standard deviation of the measurements to determine the 95- % CI.
95 % CI = 95 % confidence interval.
95 % CI = $\pm \dfrac{ts}{\sqrt{n}}$

% RA = % relative accuracy.
% RA = $\dfrac{95\ \%\ CI}{\bar{X}} \times 100$

$SB_{\perp}$ = mean center-to-center spacing of the bands.
$SB_{\perp}$ = $\dfrac{1}{\bar{N}_{L\perp}}$.

V_V = volume fraction of the banded phase (constituent).

$\lambda_{\perp}$ = mean edge-to-edge spacing of the bands, mean free path (distance).
$\lambda_{\perp}$ = $\dfrac{1 - V_V}{\bar{N}_{L\perp}}$

AI = anisotropy index.
AI = $\dfrac{\bar{N}_{L\perp}}{\bar{N}_{L||}} = \dfrac{\bar{P}_{L\perp}}{\bar{P}_{L||}}$

Ω_{12} = degree of orientation of partially oriented linear structure elements on the two-dimensional plane-of-polish.

$$\Omega_{12} = \frac{\bar{N}_{L\perp} - \bar{N}_{L\parallel}}{\bar{N}_{L\perp} + 0.571\,\bar{N}_{L\parallel}}$$

$$\Omega_{12} = \frac{\bar{P}_{L\perp} - \bar{P}_{L\parallel}}{\bar{P}_{L\perp} + 0.571\,\bar{P}_{L\parallel}}$$

4. Summary of Practice

4.1 The degree of microstructural banding or orientation is described qualitatively using metallographic specimens aligned parallel to the deformation direction of the product.

4.2 Stereological methods are used to measure the number of bands per unit length, the inter-band or interparticle spacing and the degree of anisotropy or orientation.

4.3 Microindentation hardness testing is used to determine the hardness of each type band present in hardened specimens and the difference in hardness between the band types.

5. Significance and Use

5.1 This practice is used to assess the nature and extent of banding or orientation of microstructures of metals and other materials where deformation and processing produce a banded or oriented condition.

5.2 Banded or oriented microstructures can arise in single phase, two phase or multiphase metals and materials. The appearance of the orientation or banding is influenced by processing factors such as the solidification rate, the extent of segregation, the degree of hot or cold working, the nature of the deformation process used, the heat treatments, and so forth.

5.3 Microstructural banding or orientation influence the uniformity of mechanical properties determined in various test directions with respect to the deformation direction.

5.4 The stereological methods can be applied to measure the nature and extent of microstructural banding or orientation for any metal or material. The microindentation hardness test procedure should only be used to determine the difference in hardness in banded heat-treated metals, chiefly steels.

5.5 Isolated segregation may also be present in an otherwise reasonably homogeneous microstructure. Stereological methods are not suitable for measuring individual features, instead use standard measurement procedures to define the feature size. The microindentation hardness method may be used for such structures.

5.6 Results from these test methods may be used to qualify material for shipment in accordance with guidelines agreed upon between purchaser and manufacturer, for comparison of different manufacturing processes or process variations, or to provide data for structure-property-behavior studies.

6. Apparatus

6.1 A metallurgical (reflected-light) microscope is used to examine the microstructure of test specimens. Banding or orientation is best observed using low magnifications, for example, 50× to 200×.

6.2 Stereological measurements are made by superimposing a test grid (consisting of a number of closely spaced parallel lines of known length) on the projected image of the microstructure or on a photomicrograph. Measurements are made with the test lines parallel and perpendicular to the deformation direction. The total length of the grid lines should be at least 500 mm.

6.3 These stereological measurements may be made using a semiautomatic tracing type image analyzer. The test grid is placed over the image projected onto the digitizing tablet and a cursor is used for counting.

6.4 For certain microstructures where the contrast between the banded or oriented constituents is adequate, an automatic image analyzer may be used for counting, where the TV scan lines for a live image, or image convolutions[5], electronically-generated test grids[6], or other methods, for a digitized image, are used rather than the grid lines of the plastic overlay or reticle.

6.5 A microindentation hardness tester is used to determine the hardness of each type of band in heat-treated steels or other metals. The Knoop indenter is particularly well suited for this work.

7. Sampling and Test Specimens

7.1 In general, specimens should be taken from the final product form after all processing steps have been performed, particularly those that would influence the nature and extent of banding. Because the degree of banding or orientation may vary through the product cross section, the test plane should sample the entire cross section. If the section size is too large to permit full cross sectioning, samples should be taken at standard locations, for example, subsurface, mid-radius (or quarter-point), and center, or at specific locations based upon producer-purchaser agreements.

---

[5] Lépine, M., "Image Convolutions and their Application to Quantitative Metallography," **Microstructural Science,** Vol. 17, **Image Analysis and Metallography**, ASM International, Metals Park, OH, 1989, pp. 103–114.

[6] Fowler, D.B., "A Method for Evaluating Plasma Spray Coating Porosity Content Using Stereological Data Collected by Automatic Image Analysis," **Microstructural Science**, Vol. 18, **Computer-Aided Microscopy and Metallography**, ASM International, Materials Park, OH, 1990, pp. 13–21.

7.2 The degree of banding or orientation present is determined using longitudinal test specimens, that is, specimens where the plane of polish is parallel to the deformation direction. For plate or sheet products, a planar oriented (that is, polished surface parallel to the surface of the plate or sheet) test specimen, at subsurface, mid-thickness, or center locations, may also be prepared and tested depending on the nature of the product application.

7.3 Banding or orientation may also be assessed on intermediate product forms, such as billets or bars, for material qualification or quality control purposes. These test results, however, may not correlate directly with test results on final product forms. Test specimens should be prepared as described in 7.1 and 7.2 but with the added requirement of choosing test locations with respect to ingot or continuously cast slab/strand locations. The number and location of such test specimens should be defined by producer-purchaser agreement.

7.4 Individual metallographic test specimens should have a polished surface area covering the entire cross section if possible. The length of full cross-section samples, in the deformation direction, should be at least 10 mm (0.4 in.). If the product form is too large to permit preparation of full cross sections, the samples prepared at the desired locations should have a minimum polished surface area of 100 mm^2(0.16 in. ^{2}) with the sample length in the longitudinal direction at least 10 mm (0.4 in.).

8. Specimen Preparation

8.1 Metallographic specimen preparation should be performed in accordance with the guidelines and recommended practices given in Methods E 3. The preparation procedure must reveal the microstructure without excessive influence from preparation-induced deformation or smearing.

8.2 Mounting of specimens may be performed depending on the nature of the test sample or if needed to accommodate automatic polishing devices.

8.3 The microstructure should be revealed in strong contrast by any appropriate chemical or electrolytic etching method, by tinting or staining, etc. Test Methods E 407 list appropriate etchants for most metals and alloys. For certain materials, etching may not be necessary as the naturally occurring reflectivity differences between the constituents may produce adequate contrast.

9. Calibration

9.1 Use a stage micrometer to determine the magnification of the projected image or at the photographic plane.

9.2 Use a ruler to determine the length of the test lines on the grid overlay in mm.

10. Procedure

10.1 Place the polished and etched specimen on the microscope stage, select a suitable low magnification, for example, 50× or 100×, and examine the microstructure. Align the specimen so that the deformation direction is horizontal on the projection screen. Randomly select the initial field by arbitrarily moving the stage and accepting the new field without further stage adjustment.

10.1.1 Bright field illumination will be used for most measurements. However, depending on the alloy or material being examined, other illumination modes, such as polarized light or differential interference contrast illumination, may be used.

10.1.2 Measurements may also be made by placing the test grid on photomicrographs (see Guide E 883), taken of randomly selected fields, at suitable magnifications.

10.2 Qualitatively define the nature and extent of the banding or orientation present in accordance with the following guidelines. Examination at higher magnification may be required to identify and classify the constituents present. Fig. 2 describes the classification approach.

10.2.1 Determine if the banding or orientation present represents variations in the etch intensity of a single phase or constituent, such as might result from segregation in a tempered martensite alloy steel specimen, or is due to preferential alignment of one or more phases or constituents in a two-phase or multi-phase specimen.

10.2.2 For orientation or banding in a two-phase or multi-phase specimen, determine if only the minor phase or constituent is preferentially aligned within the matrix phase. Alternatively, both phases may be aligned with neither appearing as a matrix phase.

10.2.3 For two-phase (constituent) or multiphase (constituent) microstructures, determine if the aligned second phase (constituent) is banded in a layered manner or exists in an oriented, non-banded, randomly distributed manner.

10.2.4 For cases where a second phase or constituent is banded or oriented within a non-banded, nonoriented matrix, determine if the banded or oriented constituent exists as discrete particles (the particles may be globular or elongated) or as a continuously aligned constituent.

10.2.5 Describe the appearance of the distribution of the second phase (or, either lighter or darker etching regions within a single phase microstructure) in terms of the pattern present, for example: isotropic (nonoriented or non-banded), nearly isotropic, partially banded, partially oriented, diffusely banded, narrow bands, broad bands, mixed narrow and broad bands, fully oriented, etc.

10.2.6 The microstructural examples presented in Annex A1 illustrate the use of such terminology to provide a qualitative description of the nature and extent of the banding or orientation. Fig. 2 describes the classification approach.

10.3 Place the grid lines over the projected image or photomicrograph of the randomly selected field (see section 10.17) so that the grid lines are perpendicular to the deformation direction. The grid should be placed without operator bias. Decide which phase or constituent is banded. If both phases or constituents are banded, with no obvious matrix phase, choose one of the phases (constituents) for counting. Generally, it is best to count the banded phase present in least amount. Either N_L or P_L, or both (see

10.3.1-10.3.4 for definitions), may be measured, using grid orientations perpendicular (⊥) and parallel (||) to the deformation direction, depending on the purpose of the measurements or as required by other specifications.

10.3.1 *Measurement of* $N_{L\perp}$—with the test grid perpendicular to the deformation direction, count the number of discrete particles or features intercepted by the test lines. For a two-phase structure, count all of the interceptions of the phase of interest, that is, those that are clearly part of the bands and those that are not. When two or more contiguous particles, grains, or patches of the phase or constituent of interest are crossed by the grid line, that is, none of the other phase or constituent is present between the like particles, grains, or patches, count them as one interception ($N = 1$). Tangent hits are counted as one half an interception. If a line ends within a particle, patch or grain, count it as one half an interception. Table 1 provides rules for counting while Fig. 1 illustrates the counting procedure. Calculate the number of feature interceptions per unit length perpendicular to the deformation axis, $N_{L\perp}$, in accordance with:

$$N_{L\perp} = \frac{N_{\perp}}{L_t} \tag{1}$$

where:

$N_{\perp}$ = number of interceptions and

L_t = true test line length in mm, that is, the length of the grid lines in mm divided by the magnification, M.

10.3.2 *Measurement of* $N_{L\parallel}$—Rotate the test grid over the same field and location measured for N_L so that the test lines are oriented parallel to the deformation direction. Do not deliberately orient the grid lines over any particular microstructural feature or features. Count all of the feature interceptions, $N_{\parallel}$, with the test lines (in the same way as described in 10.3.1) whether they are obviously part of the banded region or not. Calculate the number of interceptions per unit length parallel to the deformation axis, $N_{L\parallel}$, in accordance with:

$$N_{L\parallel} = \frac{N_{\parallel}}{L_t} \tag{2}$$

where:

L_t = true test line length as defined in 10.3.1.

10.3.3 *Measurement of* $P_{L\perp}$—With the test grid perpendicular to the deformation direction, count the number of times the test lines intersect a particle, phase or constituent boundary, $P_{\perp}$, whether the particle, phase or constituent is clearly part of the band or not. Do not count phase or constituent boundaries between like particles, grains, or patches. Count only phase or constituent boundary intersections between unlike particles, grains, or patches. Tangent hits are counted as one intersection. Table 1 provides rules for counting while Fig. 1 illustrates the counting procedure. Calculate the number of boundary intersections per unit length perpendicular to the deformation axis, $P_{L\perp}$, in accordance with:

$$P_{L\perp} = \frac{P_{\perp}}{L_t} \tag{3}$$

where:

L_t = true test line length as defined in 10.3.1.

10.3.4 Measurement of $P_{L\parallel}$—Rotate the test grid over the same field and location measured for P_L so that the lines are oriented parallel to the deformation direction and count the number of all particle, phase, or constituent boundary intersections, $P_{\parallel}$, with the test line for the feature of interest (in the same ways as described in 10.3.3). Calculate the number of boundary intersections per unit test length parallel to the deformation axis, $P_{L\parallel}$, in accordance with:

TABLE 1 Rules for N and P Counts

NOTE 1—Fig. 1 illustrates some of these counting rules.

1.	*N Interceptions*—Count the number of individual particles, grains, or patches of the constituent of interest crossed by the grid lines.
2.	*P Intersections*—Count the number of unlike phase boundaries or constituent boundaries[A] crossed by the grid lines.
3.	If two or more contiguous particles, grains, or patches of the phase or constituent of interest are crossed by the grid lines (none of the other phase or constituent between the particles where crossed) count them as one particle intercepted ($N = 1$). For *P* intersections, do not count phase or constituent boundaries between like particles, grains, etc. This problem occurs most commonly in $N_{L\parallel}$ and $P_{L\parallel}$ measurements in highly banded structures.
4.	When a test line is tangent to the particle, grain, or patch of interest, *N* is counted as ½ and *P* as 1.
5.	If a test line ends within a particle, count *N* as ½ and *P* as 1.
6.	If the entire test line lies completely within the phase or feature of interest (this can occur for parallel counts of a highly banded material), count *N* as ½ and *P* as 0.

[A] If possible, etch the specimens so that like phase or constituent boundaries are not revealed, only unlike boundaries.

$$P_{L\parallel} = \frac{P_{\parallel}}{L_t} \tag{4}$$

where:
L_t = true test line length as defined in 10.3.1.

10.3.5 These measurements should be repeated on at least five fields per sample or location, each selected without operator bias. If the banded condition appears to vary substantially across the longitudinal section, measurements may be made at specific locations, for example, subsurface, midthickness and center locations, or at a series of locations across the thickness to assess the positional variability.

10.3.6 Examples of the use of these measurement procedures are given in Annex A1.

10.4 For banded heat-treated microstructures, particularly for alloy steels, the above microstructural measurements may be supplemented by determination of the average microindentation hardness of the bands. Determine the nature of the banding present, for example, light versus dark etching martensite or bainite versus martensite.

10.4.1 Knoop-type indents are made in each band. The load is adjusted so that the indent can be kept completely within the bands. If possible, a 500 gf load should be used, particularly if the equivalent Rockwell C hardness (HRC) is to be estimated. Tests should be conducted according to the guidelines given in Test Methods E 384.

10.4.2 The average hardness of at least five indents in each type of band (light vs. dark etching martensite or martensite vs. bainite, depending on the nature of the bands) should be determined. For small segregates, it may not be possible to obtain five or more hardness tests values.

NOTE 3—If the difference in Knoop hardness between the bands is not large, the statistical significance of the difference can be determined using the t-test as described in most statistics textbooks.

10.4.3 Conversion of Knoop hardness (HK) values to the equivalent Rockwell C value must be done with care and may involve considerable error, particularly if the test loads used are lower than 500 gf. Tables E140 do not provide HK to HRC (or other scales) conversions for steels with hardness above 251 HK; however, Test Methods and Definitions A 370 do provide HK to HRC conversions for the hardness range covering heat treated steels. The equations given in Annex A2 may be helpful for such conversions.

10.4.4 For as-quenched carbon and alloy steels with bulk carbon contents from 0.10 to 0.65 %, the carbon contents of the matrix and the segregate streaks or patches may be estimated from the as-quenched hardness. Both the matrix and the segregates must be fully martensitic (except for normal minor amounts of retained austenite) and in the as-quenched condition. The Knoop microindentation hardnesses (500 gf) for matrix and segregate are converted to HRC values ((Eq 1) and (Eq 3) of Annex A2) and the carbon contents are estimated using Eq 2 or Eq 4 (Annex A2), depending on the hardness level.

11. Calculation of Results

11.1 After the desired number of fields n have been measured, or the number of microindentation impressions n have been measured, calculate the mean value of each measurement made by dividing the sum of the measurements by n to determine the average values of $\bar{N}_{L\perp}$, $\bar{N}_{L\parallel}$, $\bar{P}_{L\perp}$, $\bar{P}_{L\parallel}$ or the average Knoop microindentation hardness of each type band. For a highly banded microstructure, $\bar{N}_{L\perp}$ (the bar above the quantity indicates an average value) is a measure of the number of bands per mm (one-half $\bar{P}_{L\perp}$ is approximately equal to $\bar{N}_{L\perp}$).

11.2 Next, calculate the standard deviations of these measurements for n fields or n microindentation impressions in accordance with:

$$s = \left[\frac{1}{n-1} \sum_{i=1}^{n} [X_i - \bar{X}]^2 \right]^{1/2} \tag{5}$$

where:
X_i = individual field measurements and
$\bar{X}$ = mean value.

The measured means and standard deviations can be easily calculated using most pocket calculators.

11.3 Next, calculate the 95 % confidence interval, 95 % CI, for each measurement, in accordance with:

$$95\ \%\ \text{CI} = \pm \frac{ts}{\sqrt{n}} \tag{6}$$

TABLE 2 *t* Values for Calculating 95% Confidence Intervals

NOTE 1—n is the number of measurements.

$n-1$	t	$n-1$	t
2	4.303		2.365
3	3.182	7	2.306
4	2.776	8	2.262
5	2.571	9	2.228
6	2.447	10	

where:
s = standard deviation and
t varies with the number of measurements (see Table 2).

The value of each measurement is expressed as the mean value ± the 95 % CI.

11.4 Next, calculate the % relative accuracy, % RA, of each measurement in accordance with:

$$\% \text{ RA} = \frac{95\ \%\ CI}{\bar{X}} \times 100 \tag{7}$$

where:
$\bar{X}$ = mean value of each measurement.

The relative accuracy is an estimate of the % error of each measurement as influenced by the field-to-field variability of the values. A relative accuracy of 30 % or less is generally adequate. If the % RA is substantially higher, additional measurements may be made to improve the % RA value.

11.5 The mean spacing (center-to-center) of the banded or oriented phase (constituent), $SB_{\perp}$, can be determined from the reciprocal of $\bar{N}_{L\perp}$:

$$SB_{\perp} = \frac{1}{\bar{N}_{L\perp}} \tag{8}$$

The mean free path spacing (edge-to-edge) may also be calculated. This requires a measurement of the volume fraction, V_V, of the banded or oriented phase (constituent) by point counting (see Practice E 562) or other suitable methods. The mean free path spacing, $\lambda_{\perp}$, is calculated in accordance with:

$$\lambda_{\perp} = \frac{1 - V_V}{\bar{N}_{L\perp}} \tag{9}$$

where:
V_V = is a fraction (not a percentage).

The difference between the mean spacing and the mean free path provides an estimate of the mean width of the banded or oriented phase or constituent.

11.6 Calculate the anisotropy index, AI, using the mean values determined in 11.1 as follows:

$$\text{AI} = \frac{\bar{N}_{L\perp}}{\bar{N}_{L\parallel}} \text{ or, AI} = \frac{\bar{P}_{L\perp}}{\bar{P}_{L\parallel}} \tag{10}$$

These two indexes should be approximately equal because, ignoring the influence of tangent hits and counting errors, $P_L = 2N_L$ for such structures. The anisotropy index for a randomly oriented, non-banded microstructure is one. As the degree of orientation or banding increases, the anisotropy index increases above one.

11.7 The degree of orientation, Ω_{12}, of partially oriented linear structure elements on a two-dimensional plane of polish[7] can be calculated using either the N_L or P_L values determined in 11.1 in accordance with:

$$\Omega_{12} = \frac{\bar{N}_{L\perp} - \bar{N}_{L\parallel}}{\bar{N}_{L\perp} + 0.571\,\bar{N}_{L\parallel}} \text{ or } \Omega_{12} = \frac{\bar{P}_{L\perp} - \bar{P}_{L\parallel}}{\bar{P}_{L\perp} + 0.571\,\bar{P}_{L\parallel}} \tag{11}$$

These two indexes should be approximately equal because, ignoring the influence of tangent hits and counting errors, $P_L = 2N_L$ for such structures. The degree of orientation can vary from zero (completely random distribution) to 1.0 (fully oriented).

12. Test Report

12.1 The report should document the identifying information regarding the specimens tested, their origin, location, product form, date of analysis, number of fields or indents measured, magnification used, etc.

12.2 Describe the nature and extent of the banded or oriented microstructural condition present.

12.3 Depending on the measurements performed, list the mean, standard deviation, 95 % confidence interval and % relative accuracy for each measurement ($N_{L\perp}$, $N_{L\parallel}$, $P_{L\perp}$, $P_{L\parallel}$, and HK for each type band). Next, depending on the measurements performed, list the anisotropy index (or indexes), AI, calculated in 11.6 and the degree of orientation value (or values), Ω_{12}, calculated in 11.7. For highly banded microstructures, list the spacing values $SB_{\perp}$ and $\lambda_{\perp}$, calculated in 11.5.

12.4 For specimens where the microindentation hardness of the bands was determined, calculate the difference in Knoop hardness between the bands, if desired. Conversion of HK values to HRC (or other scales) may involve considerable error (particularly for test loads below 500 gf). The conversion chart in Test Methods and Definitions A 370, or the equations in Annex A2, should be used.

12.4.1 For as-quenched carbon and alloy steels with martensitic matrixes and martensitic segregation, the carbon contents of the matrix and segregate can be estimated from the as-quenched hardnesses using the procedure described in Annex A2. This

[7] E. E. Underwood, *Quantitative Stereology*, Addison-Wesley Publishing Co., Inc., Reading, MA, 1970.

method is applicable only to steels with carbon contents from 0.10 to 0.65 % and both segregate and matrix must be martensitic. The degree of carbon segregation may be estimated by this method and reported for such specimens.

13. Precision and Bias

13.1 There are no standards that can be used to rigorously define the precision of banding measurements and detect bias.

13.2 Because banding is detected on longitudinally oriented metallographic specimens taken parallel to the deformation direction, deviations of the plane of polish of more than about 5° will influence measurement results.

13.3 Improper specimen preparation will influence test results. Etching must produce strong contrast between the phases or constituents of interest. It is best if the etchant used does not reveal grain boundaries within a given phase.

13.4 The degree of banding or alignment and the width of the bands will vary across the specimen cross section. Therefore, it is necessary to evaluate the banding or alignment characteristic at specific locations.

13.5 The magnification used can influence test results. The magnification must be high enough to permit accurate counting of feature interceptions or phase boundary intersections. However, the magnification must be kept as low as possible so that each test line traverses a reasonable number of the grains or particles of interest.

13.6 The test lines must be accurately aligned perpendicular and parallel to the deformation direction for accurate counting and determination of $N_{L\perp}$, $N_{L\parallel}$, $P_{L\perp}$ and $P_{L\parallel}$. Deviations of more than 5° from perpendicular or parallel must be avoided.

13.7 In general, as the number of fields measured increases, the statistical variability of the test results decreases. The relative accuracy of test measurements parallel to the hot-working axis is nearly always poorer than for measurements perpendicular to the deformation direction, as demonstrated by the test data in Annex A1. For a given number of fields measured, the statistical precision is generally better for coarse structures than for fine structures and for isotropic structures compared to highly banded or aligned structures.

13.8 The counting rules must be followed consistently, otherwise the within-laboratory and between-laboratory repeatability and reproducibility will suffer.

13.9 The verbal description of the nature of the banding or alignment is qualitative and somewhat subjective. There are presently no absolute guides between the measured quantitative parameters and the qualitative terms used to describe the microstructure.

13.10 The values of the anisotropy index and the degree of orientation cannot be used to establish whether the microstructure is merely oriented parallel to the deformation direction or is actually banded. This difference requires pattern recognition techniques which are beyond the scope of this method. However, an experienced operator can distinguish between the two forms of alignment, perhaps aided by the examples in Annex A1.

13.11 The microindentation hardness procedure for defining the difference in hardness between bands is subject to those factors that influence the precision and bias of such test results (see Test Method E 384).

13.12 Conversion of 500 gf Knoop hardness results to HRC values introduces another source of uncertainty which is difficult to define.

13.13 Prediction of the carbon content of as-quenched fully martensitic carbon and alloy steels (matrix and segregate), or the difference in carbon content between the segregate and matrix, should be viewed as an approximation due to the variability of published data for the as-quenched hardness (100 % martensite) as a function of the carbon content of carbon and alloy steels.

14. Keywords

14.1 anisotropy index; banding; feature interceptions; feature intersections; microindention hardness; orientation; steel; stereology

ANNEXES

(Mandatory Information)

A1. EXAMPLES OF MEASUREMENTS OF BANDED OR ORIENTED MICROSTRUCTURES

A1.1 This annex provides examples of microstructures (Figs. A1.1-A1.20), both single-phase and two-phase, that illustrate various degrees of banded or oriented microstructures. Each microstructure has been qualitatively described in accordance with the scheme outlined in Fig. 1 and each has been measured using the appropriate procedures described in 10.3. All of the measurements were made using 2× enlargements of the photomicrographs presented. The grid used for these measurements consisted of eight parallel lines, spaced 20 mm (0.79 in.) apart; each line measured 125 mm (4.9 in.) long for a total line length of 1000 mm (39.4 in.). The grid was alternately aligned perpendicular and parallel to the deformation axis at various locations over the prints, selected at random with as little bias as possible. A minimum of five measurements in each direction, generally more, were made on each micrograph by one or more persons. The deformation axis in each microstructure shown is horizontal.

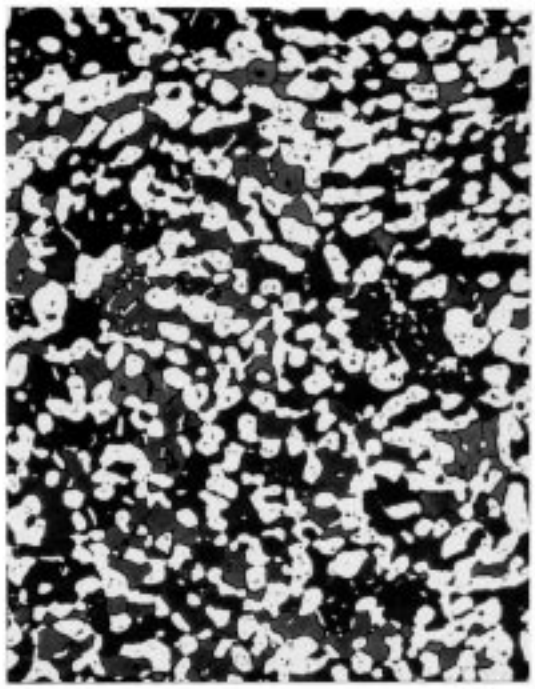

Wrought AISI 312 Stainless Steel

	$\bar{N}_{L\perp}$(No./mm)	$\bar{N}_{L\|\|}$ (No./mm)	AI $\bar{N}_{L\perp}/\bar{N}_{L\|\|}$	Ω_{12}	$\bar{P}_{L\perp}$(No./mm)	$\bar{P}_{L\|\|}$ (No./mm)	AI $\bar{P}_{L\perp}/\bar{P}_{L\|\|}$	Ω_{12}
$\bar{X}$	32.30	28.71	1.13	0.074	62.02	56.50	1.10	0.059
s	1.409	2.316			3.208	4.117		
95 % CI	±1.06	±1.75			±2.42	±3.10		
% RA	3.3	6.1			3.9	5.5		
n	10							

NOTE 1—Measurements made on the austenite (white) phase.

FIG. A1.1 Nonoriented, Non-Banded Isotropic Two-Phase Microstructure with no Matrix Phase; Ferrite (Dark), Austenite (White)

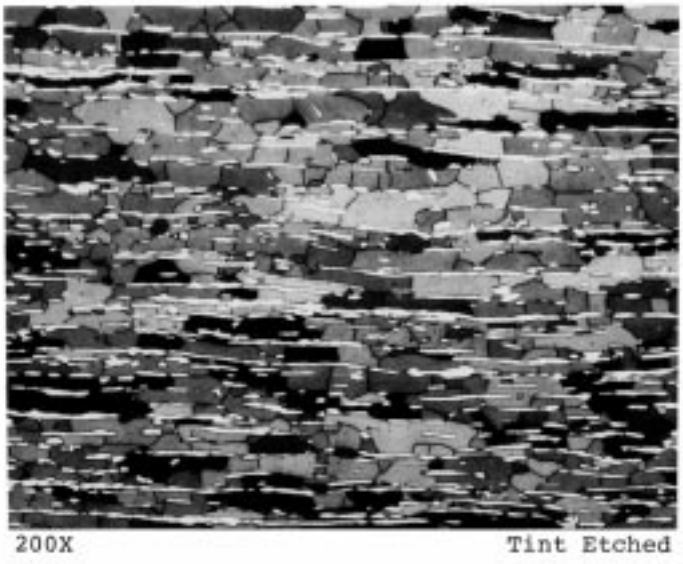

Wrought AISI 329 Stainless Steel

	$\bar{N}_{L\perp}$(No./mm)	$\bar{N}_{L\|\|}$ (No./mm)	AI $\bar{N}_{L\perp}/\bar{N}_{L\|\|}$	Ω_{12}	$\bar{P}_{L\perp}$(No./mm)	$\bar{P}_{L\|\|}$ (No./mm)	AI $\bar{P}_{L\perp}/\bar{P}_{L\|\|}$	Ω_{12}
$\bar{X}$	61.28	13.18	4.65	0.699	121.83	25.58	4.76	0.705
s	3.828	2.390			7.231	4.557		
95 % CI	±2.57	±1.61			±4.86	±3.06		
% RA	4.2	12.2			4.0	12.0		
n	11							
			$V_{V\gamma}$ = 0.227	$SB_\perp$ = 0.0163 mm	$\lambda_\perp$ = 0.0126 mm			

NOTE 1—Measurements made on the austenite (white) phase.

FIG. A1.2 Highly Oriented, Banded Two-Phase Microstructure; Oriented Austenite (White) in an Oriented, Banded Ferrite (Gray to Black) Matrix

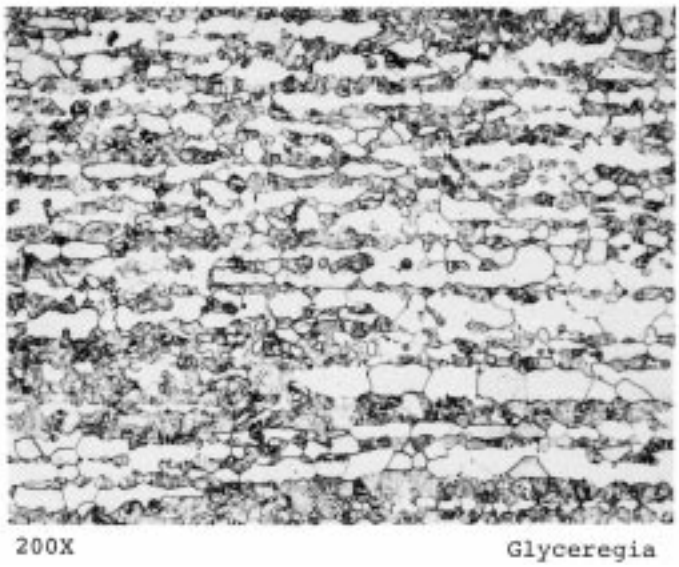

	$\bar{N}_{L\perp}$(No./mm)	$\bar{N}_{L\parallel}$(No./mm)	AI $\bar{N}_{L\perp}/\bar{N}_{L\parallel}$	Ω_{12}	$\bar{P}_{L\perp}$(No./mm)	$\bar{P}_{L\parallel}$(No./mm)	AI $\bar{P}_{L\perp}/\bar{P}_{L\parallel}$	Ω_{12}
$\bar{X}$	36.14	17.00	2.13	0.417	72.59	34.08	2.13	0.419
s	4.149	3.348			8.624	7.009		
95 % CI	±2.40	±1.93			±4.98	±4.05		
% RA	6.63	11.4			6.9	11.9		
n	14							
			$V_{V\delta}$ = 0.490	$SB_\perp$ = 0.0277 mm	$\lambda_\perp$ = 0.0141 mm			

NOTE 1—Measurements made on the delta ferrite (white) phase.

FIG. A1.3 Two-Constituent Microstructure of Oriented, Slightly Elongated, Partially Banded (Wide Bands) Delta Ferrite (White) in a Nonoriented, Non-Banded Tempered Martensite (Dark) Matrix

Differential Interference Contrast

Wrought α/βBrass (Cu-40 wt % Zn)

	$\bar{N}_{L\perp}$ (No./mm)	$\bar{N}_{L\parallel}$ (No./mm)	AI $\bar{N}_{L\perp}/\bar{N}_{L\parallel}$	Ω_{12}	$\bar{P}_{L\perp}$ (No./mm)	$\bar{P}_{L\parallel}$ (No./mm)	AI $\bar{P}_{L\perp}/\bar{P}_{L\parallel}$	Ω_{12}
$\bar{X}$	21.95	12.77	1.72	0.314	43.67	24.95	1.75	0.323
s	2.53	1.839			4.956	4.135		
95 % CI	±1.94	±1.41			±3.81	±3.18		
% RA	8.9	11.1			8.7	12.7		
n	9							

NOTE 1—Measurement made on the beta phase.

FIG. A1.4 Two-Phase Microstructure of Partially Oriented, Lightly Banded Beta Phase (in relief) in a Nonoriented, Lightly Banded Alpha-Phase Matrix (Note annealing twins.)

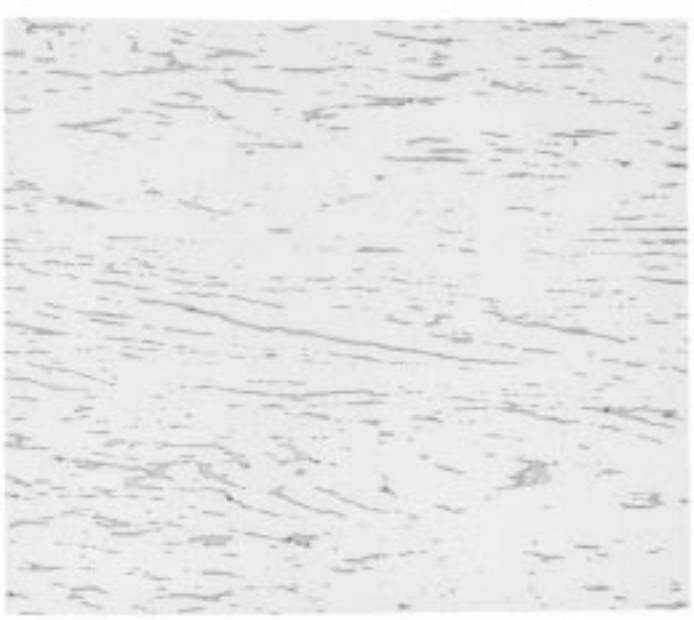

17-4PH Stainless Steel

	$\bar{N}_{L\perp}$(No./mm)	$\bar{N}_{L\parallel}$ (No./mm)	AI $\bar{N}_{L\perp}/\bar{N}_{L\parallel}$	Ω_{12}	$\bar{P}_{L\perp}$(No./mm)	$\bar{P}_{L\parallel}$ (No./mm)	AI $\bar{P}_{L\perp}/\bar{P}_{L\parallel}$	Ω_{12}
$\bar{X}$	9.47	2.32	4.08	0.662	18.31	4.47	4.10	0.663
s	0.611	0.359			1.287	0.795		
95 % CI	±0.76	±0.45			±1.6	±0.99		
% RA	8.0	19.4			8.7	22.1		
n	5							

NOTE 1—Measurements made on the delta ferrite phase.

FIG. A1.5 Two-Constituent Microstructure of Oriented, Elongated, Partially Banded Delta Ferrite (Dark) in a Nonoriented, Non-Banded Martensitic (Unetched) Matrix

17-4PH Stainless Steel

	$\bar{N}_{L\perp}$ (No./mm)	$\bar{N}_{L\parallel}$ (No./mm)	AI $\bar{N}_{L\perp}/\bar{N}_{L\parallel}$	Ω_{12}	$\bar{P}_{L\perp}$ (No./mm)	$\bar{P}_{L\parallel}$ (No./mm)	AI $\bar{P}_{L\perp}/\bar{P}_{L\parallel}$	Ω_{12}
$\bar{X}$	8.67	1.27	6.83	0.788	16.8	2.42	6.94	0.791
s	1.154	0.529			2.143	1.01		
95 % CI	±1.43	±0.66			±2.66	±1.25		
% RA	16.5	52.0			15.8	51.7		
n	5							

NOTE 1—Measurements made on the delta ferrite phase.

FIG. A1.6 Two-Constituent Microstructure of Oriented, Elongated, Partially Banded Delta Ferrite (Dark) in a Nonoriented, Non-Banded Martensitic (Unetched) Matrix

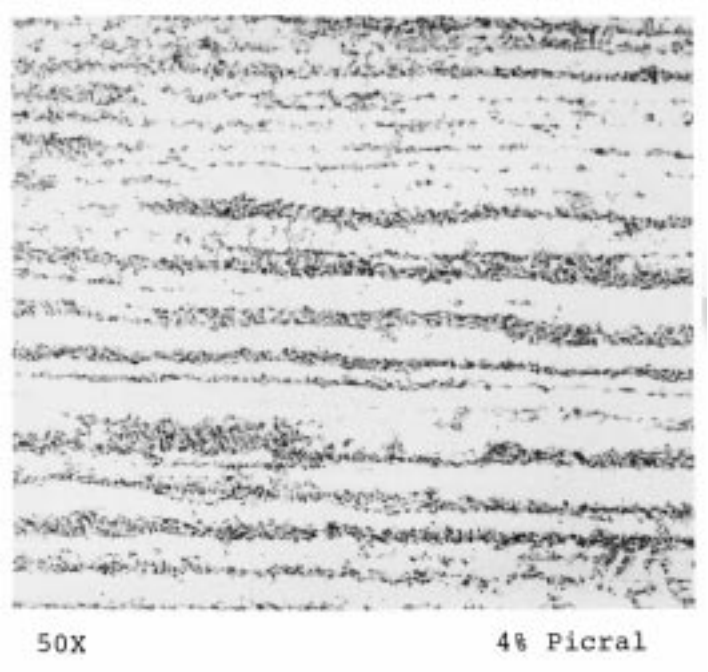

AISI 8715 Alloy Steel

	$\bar{N}_{L\perp}$ (No./mm)	$\bar{N}_{L\parallel}$ (No./mm)	AI $\bar{N}_{L\perp}/\bar{N}_{L\parallel}$	Ω_{12}	$\bar{P}_{L\perp}$ (No./mm)	$\bar{P}_{L\parallel}$ (No./mm)	AI $\bar{P}_{L\perp}/\bar{P}_{L\parallel}$	Ω_{12}	$SB_{\perp}$ (mm)	$\lambda_{\perp}$ (mm)
$\bar{X}$	8.50	2.83	3.0	0.561	17.00	5.66	3.0	0.561	0.118	0.086
s	0.4555	0.6506			0.911	1.3012				
95 % CI	±0.57	±0.81			±1.13	±1.62				
% RA	6.7	28.5			6.7	28.5				
n	5									

NOTE 1—Measurements made on the bainitic constituent.

FIG. A1.7 Two-Constituent Microstructure of Banded Upper Bainite (Dark) in a Banded, Equiaxed Ferrite (Unetched) Matrix

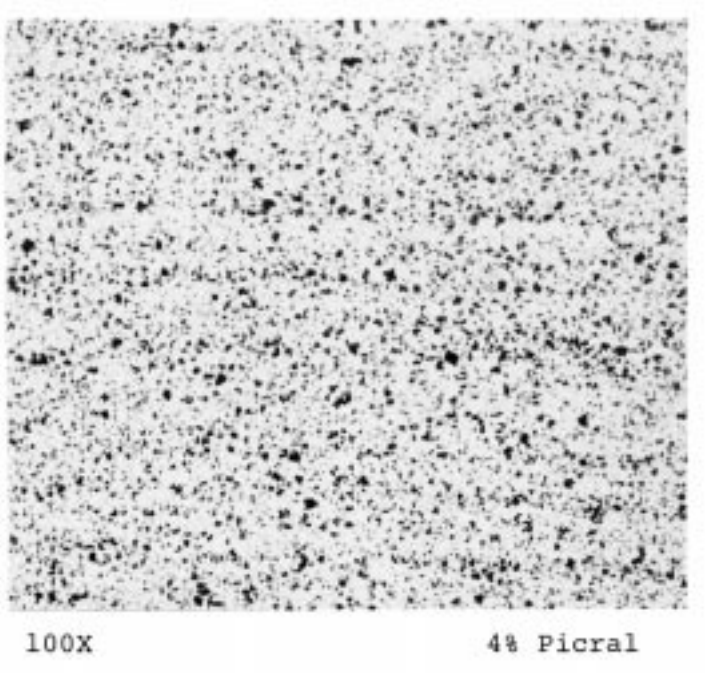

AISI 8620 Alloy Steel

	$\bar{N}_{L\perp}$(No./mm)	$\bar{N}_{L\|\|}$ (No./mm)	AI $\bar{N}_{L\perp}/\bar{N}_{L\|\|}$	Ω_{12}	$\bar{P}_{L\perp}$(No./mm)	$\bar{P}_{L\|\|}$ (No./mm)	AI $\bar{P}_{L\perp}/\bar{P}_{L\|\|}$	Ω_{12}
$\bar{X}$	28.86	25.92	1.11	0.067	56.31	52.55	1.08	0.047
s	1.6373	2.5308			4.205	4.6425		
95 % CI	±1.72	±2.66			±4.41	±4.87		
% RA	6.0	10.3			7.8	9.3		
n	6							

NOTE 1—Measurements made on the pearlitic constituent.

FIG. A1.8 Two-Constituent Microstructure with a Nearly Isotropic Distribution of Globular Patches of Pearlite (Dark) in an Equiaxed Ferrite (Unetched) Matrix

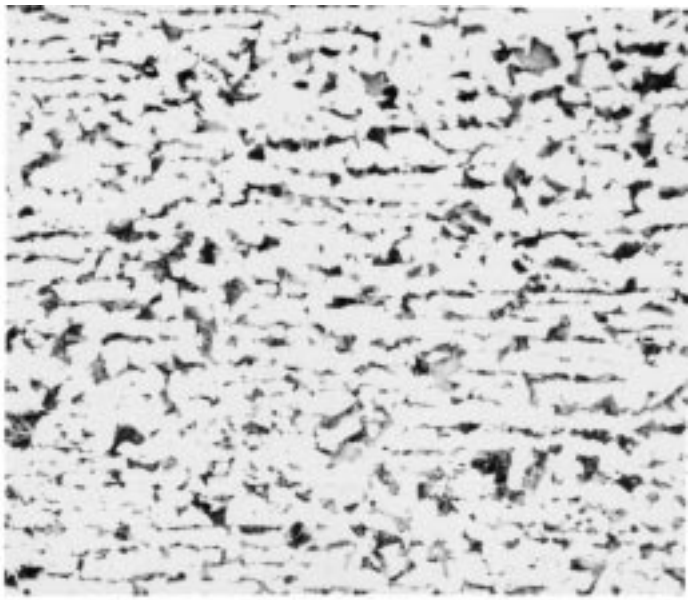

ASTM A 588/A 588M Plate Steel

	$\bar{N}_{L\perp}$ (No./mm)	$\bar{N}_{L\parallel}$ (No./mm)	AI $\bar{N}_{L\perp}/\bar{N}_{L\parallel}$	Ω_{12}	$\bar{P}_{L\perp}$ (No./mm)	$\bar{P}_{L\parallel}$ (No./mm)	AI $\bar{P}_{L\perp}/\bar{P}_{L\parallel}$	Ω_{12}	$SB_{\perp}$ (mm)	$\lambda_{\perp}$ (mm)
$\bar{X}$	39.75	25.05	1.587	0.272	80.26	49.48	1.62	0.284	0.025	0.020
s	2.323	1.807			4.961	3.664				
95 % CI	±1.94	±1.51			±4.15	±3.06				
% RA	4.9	6.0			5.2	6.2				
n	8									

NOTE 1—Measurements made on the pearlitic constituent.

FIG. A1.9 Two-Constituent Microstructure of Partially Elongated, Lightly Banded Pearlite (Dark) in an Equiaxed, Lightly Banded Ferrite (Unetched) Matrix

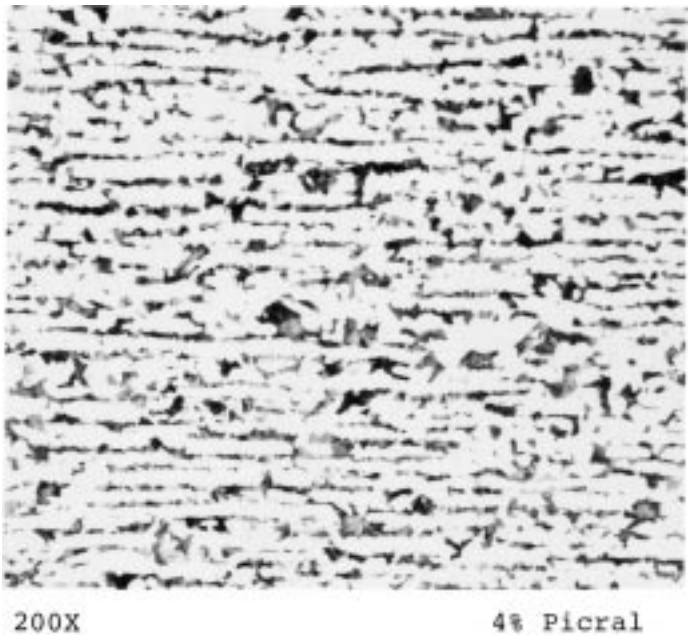

ASTM A 572/A 572M Plate Steel

	$\bar{N}_{L\perp}$ (No./mm)	$\bar{N}_{L\parallel}$ (No./mm)	AI $\bar{N}_{L\perp}/\bar{N}_{L\parallel}$	Ω_{12}	$\bar{P}_{L\perp}$ (No./mm)	$\bar{P}_{L\parallel}$ (No./mm)	AI $\bar{P}_{L\perp}/\bar{P}_{L\parallel}$	Ω_{12}	$SB_{\perp}$ (mm)	$\lambda_{\perp}$ (mm)
$\bar{X}$	51.69	26.96	1.92	0.369	101.58	53.16	1.91	0.367	0.019	0.014
s	2.688	3.189			5.793	6.923				
95 % CI	±1.71	±2.03			±3.68	±4.40				
% RA	3.3	7.5			3.6	8.3				
n	12									

NOTE 1—Measurements made on the pearlitic constituent.

FIG. A1.10 Two-Constituent Microstructure of Oriented, Partly Elongated, Predominantly Banded Pearlite (Dark) in a Banded, Equiaxed, Ferrite (Unetched) Matrix

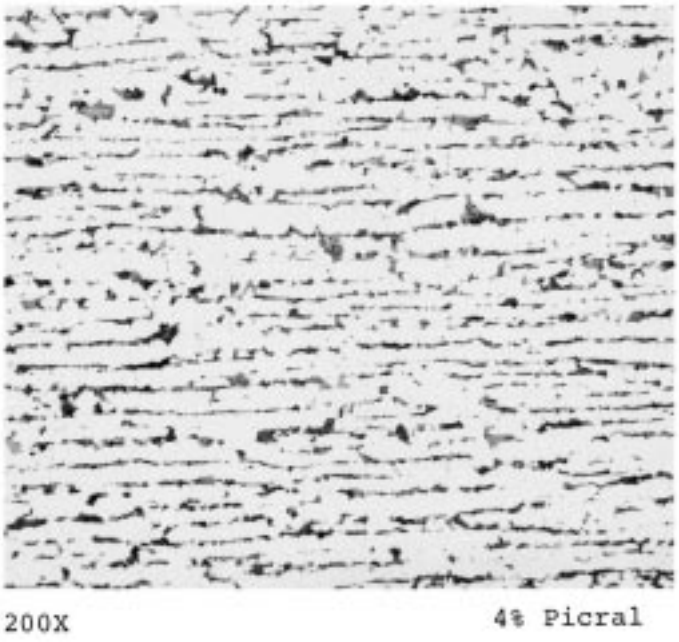

ASTM A 572/A 572M Plate Steel (Low Carbon)

	$\bar{N}_{L\perp}$ (No./mm)	$\bar{N}_{L\parallel}$ (No./mm)	AI $\bar{N}_{L\perp}/\bar{N}_{L\parallel}$	Ω_{12}	$\bar{P}_{L\perp}$ (No./mm)	$\bar{P}_{L\parallel}$ (No./mm)	AI $\bar{P}_{L\perp}/\bar{P}_{L\parallel}$	Ω_{12}	$SB_{\perp}$ (mm)	$\lambda_{\perp}$ (mm)
$\bar{X}$	51.12	16.96	3.01	0.562	99.20	33.62	2.95	0.554	0.020	0.0166
s	5.025	2.47			5.909	5.068				
95 % CI	±3.59	±1.77			±4.23	±3.63				
% RA	7.0	10.4			4.3	10.8				
n	10									

NOTE 1—Measurements made on the pearlitic constituent.

FIG. A1.11 Two-Constituent Microstructure of Oriented, Mostly Elongated, Fully Banded (Narrow Bands) Pearlite (Dark) in a Banded, Equiaxed Ferrite (Unetched) Matrix

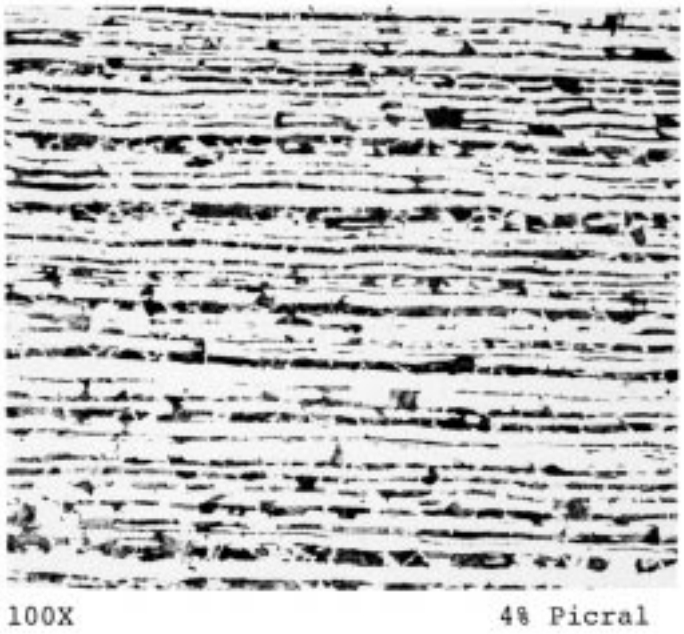

X42 Line Pipe Steel

	$\bar{N}_{L\perp}$ (No./mm)	$\bar{N}_{L\parallel}$ (No./mm)	AI $\bar{N}_{L\perp}/\bar{N}_{L\parallel}$	Ω_{12}	$\bar{P}_{L\perp}$ (No./mm)	$\bar{P}_{L\parallel}$ (No./mm)	AI $\bar{P}_{L\perp}/\bar{P}_{L\parallel}$	Ω_{12}	$SB_{\perp}$(mm)	$\lambda_{\perp}$(mm)
$\bar{X}$	37.22	9.70	3.84	0.644	73.83	18.75	3.92	0.652	0.0269	0.0195
s	2.054	2.108			4.475	4.126				
95 % CI	±1.47	±1.51			±3.20	±2.95				
% RA	3.9	15.6			4.3	15.7				
n	10									

NOTE 1—Measurements made on the pearlitic constituent.

FIG. A1.12 Two-Constituent Microstructure of Elongated, Fully Banded (Mixed Narrow and Medium Bands) Pearlite in an Elongated, Fully Banded Ferrite (Unetched) Matrix

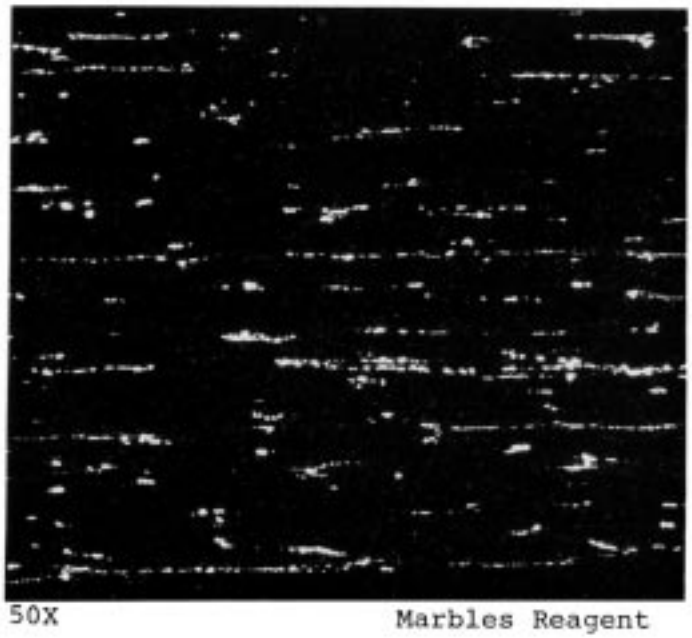

AISI M50 Bearing Steel

	$\bar{N}_{L\perp}$(No./mm)	$\bar{N}_{L\|\|}$ (No./mm)	AI $\bar{N}_{L\perp}/\bar{N}_{L\|\|}$	Ω_{12}	$\bar{P}_{L\perp}$(No./mm)	$\bar{P}_{L\|\|}$ (No./mm)	AI $\bar{P}_{L\perp}/\bar{P}_{L\|\|}$	Ω_{12}
$\bar{X}$	3.79	2.56	1.48	0.234	7.30	4.98	1.47	0.229
s	0.4823	0.770			0.9725	1.4812		
95 % CI	±0.51	±0.81			±1.02	±1.55		
% RA	13.5	31.6			14.0	31.1		
n	6							

NOTE 1—Measurements made on the carbides.

FIG. A1.13 Two-Constituent Microstructure of Elongated, Oriented, Lightly Banded Alloy Carbides (White) in a Non-Banded, Nonoriented Tempered Martensite (Black) Matrix

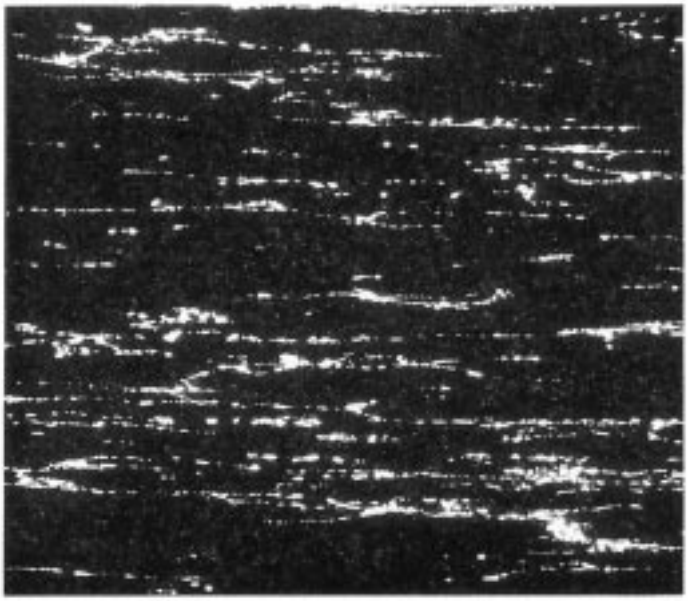

AISI M50 Bearing Steel

	$\bar{N}_{L\perp}$(No./mm)	$\bar{N}_{L\|\|}$ (No./mm)	AI $\bar{N}_{L\perp}/\bar{N}_{L\|\|}$	Ω_{12}	$\bar{P}_{L\perp}$(No./mm)	$\bar{P}_{L\|\|}$ (No./mm)	AI $\bar{P}_{L\perp}/\bar{P}_{L\|\|}$	Ω_{12}
$\bar{X}$	7.43	3.21	2.31	0.456	14.59	6.20	2.35	0.463
s	0.9778	0.7144			1.8779	1.3606		
95 % CI	±0.90	±0.66			±1.74	±1.26		
% RA	12.1	20.6			11.9	20.3		
n	7							

NOTE 1—Measurements made on the carbides.

FIG. A1.14 Two-Constituent Microstructure of Elongated, Oriented, Banded Alloy Carbides (White) in a Non-Elongated, Lightly Banded, Tempered Martensite (Black) Matrix

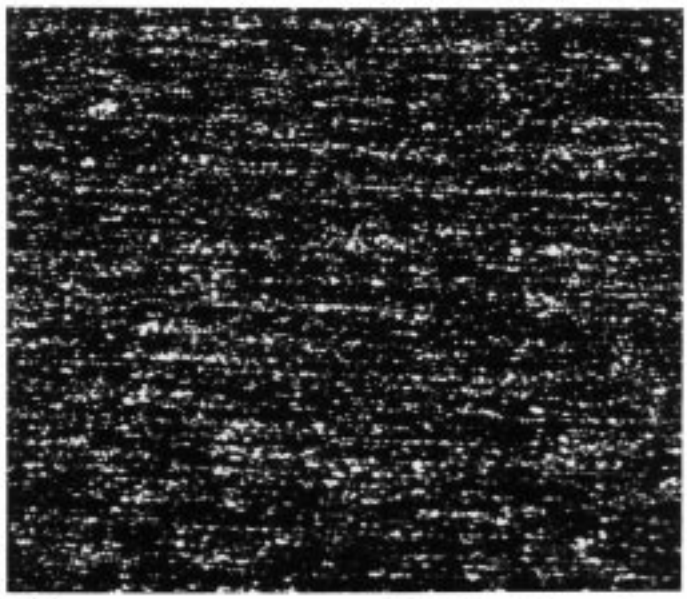

AISI 440C Stainless Steel

	$\bar{N}_{L\perp}$(No./mm)	$\bar{N}_{L\parallel}$ (No./mm)	AI $\bar{N}_{L\perp}/\bar{N}_{L\parallel}$	Ω_{12}	$\bar{P}_{L\perp}$(No./mm)	$\bar{P}_{L\parallel}$ (No./mm)	AI $\bar{P}_{L\perp}/\bar{P}_{L\parallel}$	Ω_{12}
$\bar{X}$	18.18	12.93	1.41	0.206	36.28	25.85	1.40	0.204
s	1.3253	0.7193			2.7396	1.4386		
95 % CI	±1.65	±0.89			±3.40	±1.79		
% RA	9.1	6.9			9.4	6.9		
n	5							

NOTE 1—Measurements made on the carbides.

FIG. A1.15 Two-Constituent Microstructure of Globular, Lightly Banded Alloy Carbides (White) in a Tempered Martensite (Dark) Matrix

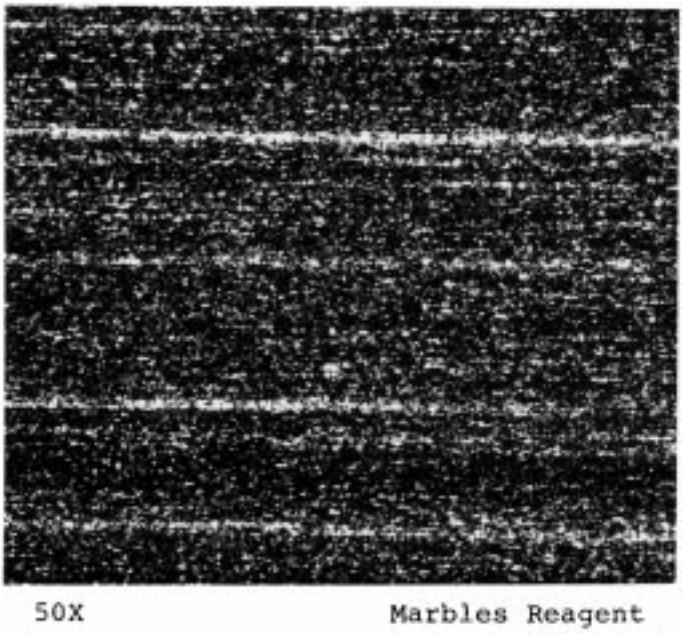

AISI 440C Stainless Steel

	$\bar{N}_{L\perp}$(No./mm)	$\bar{N}_{L\|\|}$ (No./mm)	AI $\bar{N}_{L\perp}/\bar{N}_{L\|\|}$	Ω_{12}	$\bar{P}_{L\perp}$(No./mm)	$\bar{P}_{L\|\|}$ (No./mm)	AI $\bar{P}_{L\perp}/\bar{P}_{L\|\|}$	Ω_{12}
$\bar{X}$	17.40	11.96	1.46	0.225	34.71	23.91	1.45	0.223
s	1.5952	2.8866			3.245	5.7732		
95 % CI	±1.98	±3.58			±4.03	±7.17		
% RA	11.4	30.0			11.6	30.0		
n	5							

NOTE 1—Measurements made on the carbides.

FIG. A1.16 Two-Constituent Microstructure of Globular Alloy Carbides (White) with Isolated Massive Streaks of Heavily Banded Alloy Carbides (Note massive angular carbides in streaks.) in a Tempered Martensite (Dark) Matrix

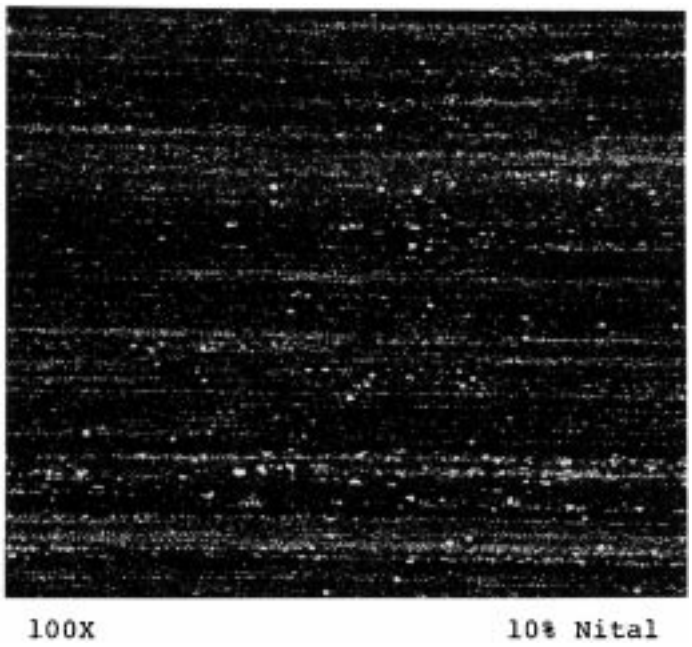

AISI M2 High Speed Steel

	$\bar{N}_{L\perp}$(No./mm)	$\bar{N}_{L\parallel}$ (No./mm)	AI $\bar{N}_{L\perp}/\bar{N}_{L\parallel}$	Ω_{12}	$\bar{P}_{L\perp}$(No./mm)	$\bar{P}_{L\parallel}$ (No./mm)	AI $\bar{P}_{L\perp}/\bar{P}_{L\parallel}$	Ω_{12}
$\bar{X}$	36.23	26.26	1.38	0.195	72.45	52.53	1.38	0.195
s	1.370	4.818			2.740	9.6358		
95 % CI	±1.70	±5.98			±3.40	±11.96		
% RA	4.7	22.8			4.7	22.8		
n	5							

NOTE 1—The carbides are more uniformly distributed in the specimen shown in Fig. A1.17 than in the specimen shown in Fig. A1.18; and, for the same number of fields measured, the values for *s*, the 95 % CI, and the % RA increase as the distribution becomes less uniform.

NOTE 2—Measurements made on the carbides.

FIG. A1.17 Two-Constituent Microstructure Consisting of Globular and Angular Lightly Banded Alloy Carbides (White) in a Tempered Martensite (Black) Matrix

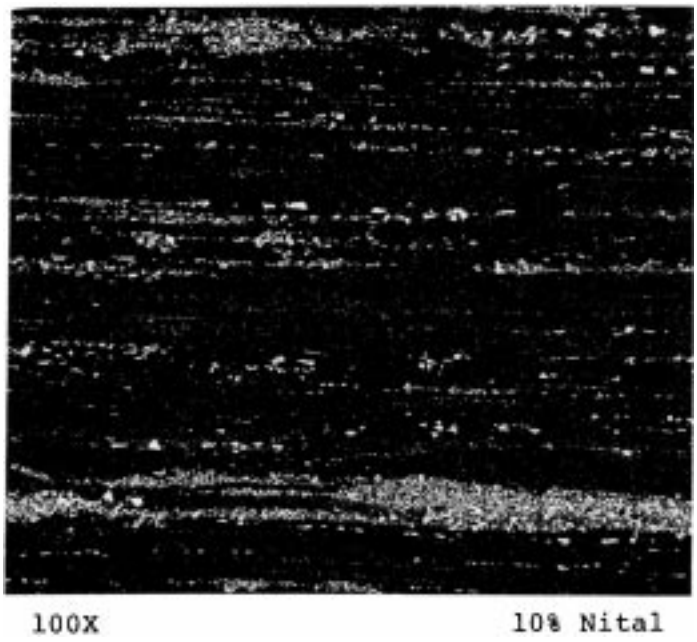

AISI M2 High Speed Steel

	$\bar{N}_{L\perp}$(No./mm)	$\bar{N}_{L\|\|}$ (No./mm)	AI $\bar{N}_{L\perp}/\bar{N}_{L\|\|}$	Ω_{12}	$\bar{P}_{L\perp}$(No./mm)	$\bar{P}_{L\|\|}$ (No./mm)	AI $\bar{P}_{L\perp}/\bar{P}_{L\|\|}$	Ω_{12}
$\bar{X}$	24.18	16.58	1.46	0.226	48.36	33.16	1.46	0.226
s	4.322	5.575			8.643	11.149		
95 % CI	±5.37	±6.92			±10.73	±13.84		
% RA	22.2	41.7			22.2	41.7		
n	5							

NOTE 1—The carbides are more uniformly distributed in the specimen shown in Fig. A1.17 than in the specimen shown in Fig. A1.18; and, for the same number of fields measured, the values for *s*, the 95 % CI, and the % RA increase as the distribution becomes less uniform.

NOTE 2—Measurements made on the carbides.

FIG. A1.18 Two-Constituent Microstructure Consisting of Globular and Angular Banded Alloy Carbides (White) with Occasional Heavy Carbide Streaks in a Tempered Martensite (Black) Matrix

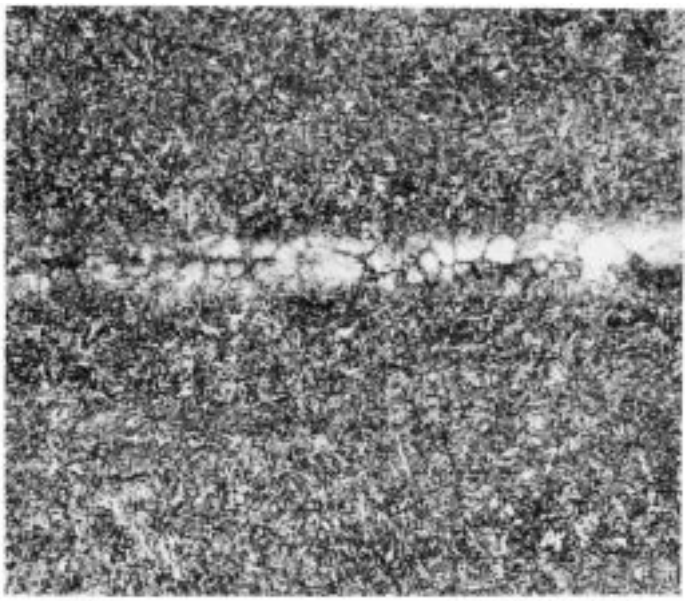

AISI 1547 Alloy Steel

	AISI 1547		
	Streaks	Matrix	ΔH
HK_{500}	774.5 ± 88.2	688.8 ± 52.4	85.7
HRC (Conv)	62.0	58.0	4.0

FIG. A1.19 Two-Constituent Microstructure Consisting of a Few Isolated Elongated Streaks of Light-Etching Martensite (White) in a Non-Banded, As-Quenched Martensite Matrix

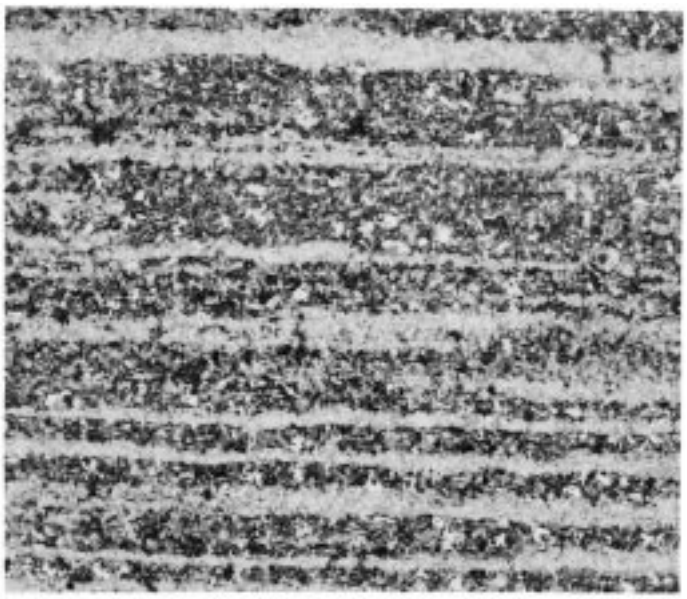

AISI 9310 Alloy Steel

AISI 9310

	Martensite				Bainite				ΔH	
	441.5 ± 21.8 43.0				320.5 ± 16.9 31.3				121.0 11.7	
	$\bar{N}_{L\perp}$(No./mm)	$\bar{N}_{L\|\|}$ (No./mm)	AI $\bar{N}_{L\perp}/\bar{N}_{L\|\|}$	Ω_{12}	$\bar{P}_{L\perp}$(No./mm)	$\bar{P}_{L\|\|}$ (No./mm)	AI $\bar{P}_{L\perp}/\bar{P}_{L\|\|}$	Ω_{12}
$\bar{X}$	5.46	0.94	5.81	0.754	10.76	1.82	5.91	0.758
s	1.156	0.251			1.883	0.473		
95 % CI	±0.89	±0.19			±1.45	±0.36		
% RA	16.3	20.5			13.5	20.0		
n	9							

NOTE 1—V_{VM} = 0.3417, $SB_{\perp}$ = 0.183 mm, and $\lambda_{\perp}$ = 0.121 mm.
NOTE 2—Measurements made on the martensite.

FIG. A1.20 Two-Constituent Microstructure of Heavily Banded (Wide Bands) Martensite (Light) in a Banded, Nonoriented Bainitic (Dark) Matrix

A2. HK TO HRC CONVERSION AND CARBON CONTENT ESTIMATION

A2.1 *Conversion of Knoop to Rockwell C:*

A2.1.1 Test Methods and Definitions A 370 list Knoop (HK) to Rockwell C (HRC) conversions for the full range of the Rockwell C test for steels. These conversions are for Knoop loads of 500 gf or greater. The accuracy of this conversion will become poorer as the test load decreases below 500 gf.

A2.1.2 A plot of this data on semilog paper (HK on log scale, HRC on linear scale) reveals a linear relationship for hardnesses ≥360 HK and 36 HRC. Linear regression for this portion of the conversion reveals the following relationship:

$$\text{HRC (converted)} = (77.6 \text{ Log HK}) - 162.2 \quad \text{(A2.1)}$$

where the correlation coefficient is 0.999908. With this equation, the predicted HRC is within ±0.17 HRC units for the range 360–480 HK and is within ±0.10 HRC for the range 495–870 HK. This small degree of error is well within the errors associated with the measurement of HK values or interpolations between chart values and should have little influence on the difference in converted HRC values for the bands. The above equation is simple to use with a pocket calculator.

A2.1.3 Because the Log HK to HRC relationship is not linear below 360 HK, the equation will predict higher HRC values if used for values ≤360 HK.

A2.1.4 For Knoop hardnesses (500 gf) below 360 HK, the following equation may be used to predict the equivalent Rockwell C hardness:

$$\text{HRC (converted)} = (103.76 \text{ Log HK}) - 228.7 \quad \text{(A2.2)}$$

This equation predicts the A 370 values within ≤0.29 HRC units over the range 342-251 HK. The correlation coefficient is 0.999448.

A2.2 *Prediction of Carbon Content from the As-Quenched Hardness:*

A2.2.1 For carbon and alloy steels with carbon contents from 0.10 to 0.65 %, there is a direct relationship between the hardness of as-quenched martensite and the carbon content. Hardenability studies have demonstrated this relationship for fully martensitic microstructures in steels rapidly quenched from the prescribed austenitizing temperatures. A plot of such data on standard rectilinear graph paper reveals two linear portions with a change of slope at 58 HRC (0.44 %C).

A2.2.2 Linear regression analysis for as-quenched hardnesses of 38 to 58 HRC (0.10–0.44 %C) reveals the following correlation equation:

$$\%C = (0.0167 \text{ HRC}) - 0.539 \quad \text{(A2.3)}$$

with a correlation coefficient of 0.9985. For as-quenched hardnesses of 58–64 HRC (0.44–0.65 %C) the following correlation equation was obtained:

$$\%C = (0.0358 \text{ HRC}) - 1.639 \quad \text{(A2.4)}$$

with a correlation coefficient of 0.9836.

A2.2.3 To illustrate the use of this relationship, the data for the AISI 1547 specimen (Fig. A1.19) will be analyzed to predict the carbon content of the matrix and the segregation streak. This specimen was in the as-quenched condition and testing revealed a Knoop microindentation hardness (500 gf) of 744.5 in the light-etching streak and 688.8 in the matrix. Using (Eq A2.2) in this Annex A2, we first convert these HK values to HRC values and obtain 62.0 HRC for the streak and 58.0 HRC for the matrix.

A2.2.4 Using (Eq A2.4), the matrix carbon content is estimated as 0.44 % while that of the light-etching streak is 0.58 %C. Note that 58 HRC is at the inflection point between the two linear portions of the HRC vs. %C relationship. If (Eq A2.3) is used to predict the carbon content of the matrix, we obtain 0.43 %C. The experimental hardenability data lists an as-quenched hardness of 58 HRC for steels with carbon contents from 0.43 to 0.45 %. Thus, there is a narrow range of uncertainty in predicting the carbon content, particularly for carbon contents of 0.44 % and higher, of about ±0.01 %C. However, this degree of uncertainty is not excessive and is less than can be achieved by micro-analytical analysis methods. This method is only applicable to as-quenched, fully martensitic steels (minor levels of retained austenite will be present in higher carbon steels) with carbon contents from 0.10 to 0.65 %.

NOTE A2.1—There is a fair degree of variability in the published relationships between the carbon content and HRC for 100 % martensite. (Eq A2.3) and (Eq A2.4) are based upon data from Sponzilli et al.[8]

[8] Sponzilli, J. T., Keith, C. J., and Walter, G. H., "Calculating Hardenability Curves from Chemical Composition," *Metal Progress*, V108, September 1975, pp. 86–87.